

Deforming the Singly Periodic Genus-One Helicoid

David Hoffman and Fusheng Wei

CONTENTS

- 1. Introduction
 - 2. The Weierstrass Representation on a Quotient Surface
 - 3. Weierstrass Data for the Helicoid as a
Screw-Motion-Invariant Surface
 - 4. Weierstrass Data for \mathcal{H}_k/σ_k
 - 5. Numerical Data and Further Results
- Acknowledgments
References

The Weierstrass data are derived—from geometric assumptions—for a family of screw-motion-invariant minimal surfaces asymptotic to the helicoid. The period problem for these data is solved numerically and the surfaces are approximated using adaptive mesh methods. These simulations give strong evidence that the family exists, is continuous, consists of embedded surfaces, and limits to the genus-one helicoid.

1. INTRODUCTION

The helicoid, \mathcal{H} , is a ruled surface that is generated by a horizontal line (the x_1 -axis, for example) sliding vertically at a constant speed up the x_3 -axis, while rotating around that axis at the same constant rate. It was proved to be a minimal surface by Meusnier in the mid-1770s. By its very definition, \mathcal{H} is embedded and singly periodic, being invariant under *vertical screw motions*: For any real number, k , the vertical screw motion, σ_k , is defined to be rotation by $2\pi k$ around the vertical axis followed by a vertical translation by $2\pi k$.

The quotient of \mathcal{H} by σ_k : (1-1)

- (i) has genus zero and two ends;
- (ii) is a portion of the helicoid that has twisted through an angle of $2\pi k$, with top and bottom edges identified;
- (iii) contains a vertical axis and is fibred by horizontal lines.

We will show strong evidence for the existence of analogs, \mathcal{H}_k , of the helicoid. These surfaces are singly periodic, embedded minimal surfaces, varying smoothly in k , whose quotients by σ_k have genus one. Animations of this family can be found at www.msri.org/publications/sgp/jim/geom/minimal/library/helicoidg1/indexc.html and in [supplement/helic1plimit/indexc.html](#).

2000 AMS Subject Classification: Primary 53A10; Secondary 53C42

Keywords: keywords here

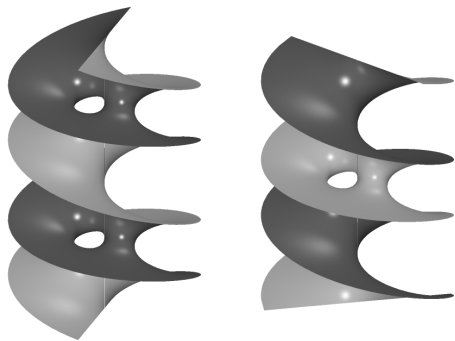


FIGURE 1. Left: The singly periodic genus one helicoid \mathcal{H}_1 . Two fundamental domains (copies of \mathcal{H}_1 modulo σ_1) are illustrated here. Right: the screw-motion invariant surface \mathcal{H}_k , for $k = 1.66$. Illustrated here is one copy of \mathcal{H}_k modulo σ_1 . See also Figure 6.

The quotient of \mathcal{H}_k by σ_k : (1-2)

- (i) has genus one and two ends;
- (ii) is asymptotic to a portion of the helicoid that has twisted through an angle of $2\pi k$;
- (iii) contains both a vertical axis, and two horizontal lines making an angle of πk with one another.

While for the helicoid any value of $k \neq 0$ is valid in (1-1), our computations indicate that the condition $k > 1/2$ is necessary for (1-2).

The ideas in this paper and the first computations date back several years. In [Hoffman et al. 99], the authors and Hermann Karcher established the existence of \mathcal{H}_1 , a translation-invariant minimal surface, and were able to prove that it is embedded. We were interested in deciding whether \mathcal{H}_1 could be perturbed. The construction and computations described in this paper show, rather convincingly, that \mathcal{H}_1 sits in a one-parameter family, \mathcal{H}_k , of minimal surfaces. (However, our construction and computations are not sufficient to prove that these surfaces actually exist and depend smoothly on the parameter k .) We were motivated to do this because we felt that the family was intrinsically important to the study of embedded minimal surfaces. Moreover, from the structure of the Weierstrass representations of the \mathcal{H}_k family, from the numerical behavior of the internal parameters as $k \rightarrow \infty$, and, most important, from the animations we made of the deformation, we were convinced that the \mathcal{H}_k family had as its limit \mathcal{H}_{e_1} , the genus one helicoid. This surface is asymptotic to the helicoid, has infinite total curvature and (of course) genus one. Together with Hermann Karcher, we proved in [Hoffman et al. 93] that

\mathcal{H}_{e_1} exists and was almost certainly embedded. There is, however, a big difference between “almost certainly” and “certainly.” Efforts to give a direct proof of the embeddedness of \mathcal{H}_{e_1} were not successful, even though many mathematicians have attempted to do so.

We knew that \mathcal{H}_1 was embedded. If the \mathcal{H}_k deformation family existed and if we were correct in asserting that the family had as its limit \mathcal{H}_{e_1} , then a relatively straightforward argument shows that the embeddedness of \mathcal{H}_1 is inherited by all the \mathcal{H}_k and passes on to \mathcal{H}_{e_1} , the genus-one helicoid. Because of the difficulty of finding a direct proof of the embeddedness of \mathcal{H}_{e_1} , understanding this family became increasingly important.

Very recently, Matthias Weber, Mike Wolf, and one of the authors gave a proof of the existence and continuity of the \mathcal{H}_k family and a limit argument that establishes the embeddedness of an \mathcal{H}_{e_1} [Weber et al. 02]. The methods are different from those described in this paper. We believe it is fair to say that the work in [Weber et al. 02] proceeds on the conviction that the \mathcal{H}_k family exists and depends continuously on k , a conviction based on the work presented in this paper.

2. THE WEIERSTRASS REPRESENTATION ON A QUOTIENT SURFACE

We present a brief overview of the Weierstrass representation, tailored to the construction of minimal surfaces invariant under screw motions. For more details, see [Hoffman and Karcher 97].

The Gauss map of a minimal surface in R^3 is an antiholomorphic map to S^2 , and the coordinate functions are harmonic with respect to the Laplace-Beltrami operator of the metric induced from R^3 . Either of these properties can be used as a definition of minimality. The metric induced from the R^3 is analytic and therefore, the underlying surface has a natural Riemann surface structure. We will refer to this Riemann surface as M .

Let g be the stereographic projection from $(0, 0, 1) \in S^2$ of its Gaussian image. Let x_3 be the coordinate function of the surface in the vertical direction, and x_3^* its (locally defined) harmonic conjugate. Define $dh := d(x_3 + ix_3^*)$. Using g and dh , it is possible to represent the minimal surface by a conformal parameterization of the form $X : M \rightarrow R^3$, where M is a Riemann surface and

$$X(p) = \operatorname{Re} \int_{p_0}^p \Phi, \tag{2-1}$$

where $\Phi = (\frac{1}{2}(1/g - g), \frac{i}{2}(1/g + g), 1)dh$, $p, p_0 \in M$.

This is one form of the Weierstrass representation of a minimal surface. One of the most important uses of (2-1) is to construct minimal surfaces from analytic data on a Riemann surface. Given an analytic function g (possibly with poles) and a holomorphic one-form dh (not necessarily closed), the immersion (2-1) is minimal with a Gauss map given by the inverse stereographic projection of g and a third coordinate given by $x_3 = \operatorname{Re} \int dh$. The immersion (2-1) will be regular, provided the induced metric is nonsingular:

$$ds = \frac{1}{2}|dh|(|g| + |g|^{-1}) \neq 0. \tag{2-2}$$

This requires the zeros of dh to coincide with (and have the same order as) the zeros and poles of g . The poles and zeros of g correspond to points where the Gauss map is vertical.

The Weierstrass representation (2-1) is, in general, multivalued. In order for (2-1) to be single-valued on M , it is necessary and sufficient that $\operatorname{Re} \int_\alpha \Phi = 0$ for all closed cycles α on M . We write this as

$$\operatorname{Re} \int_\alpha (1/g - g)dh = \operatorname{Re} \int_\alpha i(1/g + g)dh = 0$$

(Horizontal Period Condition) (2-3)

$$\operatorname{Re} \int_\alpha dh = 0 \quad (\text{Vertical Period Condition}) \tag{2-4}$$

In dealing with *periodic* minimal surfaces, it is often necessary to work with g and dh on M' , the Riemann surface of the quotient by translations or screw motions. We will be dealing with singly periodic surfaces invariant under screw motions; without loss of generality, we may assume that the translational part of the screw motion is a vertical translation and that the axis of the screw motion is the x_3 -axis. If M' is the Riemann surface of the quotient surface under screw motions, we still want the horizontal-period condition (2-3) to hold for all cycles, and we can choose a basis of cycles on M' for which the vertical-period condition (2-4) holds only on specified cycles.

When the screw motion is not a translation (i.e., when k is not an integer), we must deal with the fact that the Gauss map—and therefore g —is not in general well-defined on the quotient surface. In fact, g is defined only up to a power of $e^{2\pi ik}$. However, the one-form dg/g does descend to the quotient, and we can recover g on M' by integration:

$$g = e^{\int dg/g}. \tag{2-5}$$

Remark 2.1. Note that dg/g will have a simple pole wherever g has either a zero or a pole (corresponding to

points where the Gauss map is vertical, i.e., points where $dh = 0$), and a simple zero wherever g has a branch point.

Remark 2.2. Even though g is, in general, not well-defined on the quotient, the horizontal period condition (2-3) still makes sense. To see this, rewrite (2-3) as

$$\int_\alpha gdh = \overline{\int_\alpha 1/gdh}.$$

Here, g is a branch of the Gauss map. In this form, it is clear that substitution of $e^{i\theta}g$ for g multiplies both sides by $e^{i\theta}$.

In practice, the cycles are divided into two classes, depending on whether or not the vertical period condition (2-4) is satisfied or not. If it is, we expect that the horizontal period condition (2-3) holds, too. If it does not, then we must have $\operatorname{Re} \int_\alpha dh = 2\pi k$ and $\int_\alpha \frac{dg}{g} = 2\pi ik$ according to (2-5).

We note that the Gauss curvature and the second fundamental form of a minimal surface can be expressed in terms of the Weierstrass data g and dh . (See [Hoffman and Karcher 97, Section 2.]) :

$$K = \frac{-16}{(|g| + |g|^{-1})^4} \frac{|dg/g|^2}{|dh|^2}. \tag{2-6}$$

For a tangent vector \dot{c} to a curve $c(t)$, the second fundamental form can be expressed as the real part of a holomorphic quadratic differential:

$$B(\dot{c}, \dot{c}) = \operatorname{Re} \left(\frac{dg}{g}(\dot{c}) \cdot dh(\dot{c}) \right). \tag{2-7}$$

3. WEIERSTRASS DATA FOR THE HELICOID AS A SCREW-MOTION-INVARIANT SURFACE

As preparation for our construction of the surfaces \mathcal{H}_k , we will show that the Weierstrass data,

$$g = z^k, \quad dh = i\lambda \frac{dz}{z}, \quad \lambda \text{ real}, \quad k > 0, \tag{3-1}$$

on $M' = C - \{0\}$, when used in the Weierstrass representation (2-1), produce a minimal immersion that satisfies the conditions of (1-1).

Using (2-2), we can write the metric of this surface as

$$ds = \frac{|\lambda|}{2} (|z|^k + |z|^{-k}) \frac{|dz|}{|z|}. \tag{3-2}$$

Let $l(t) = te^{i\theta}$, $t > 0$, be a ray emanating from 0. The metric (3-2) is invariant under reflection through l (i.e.,

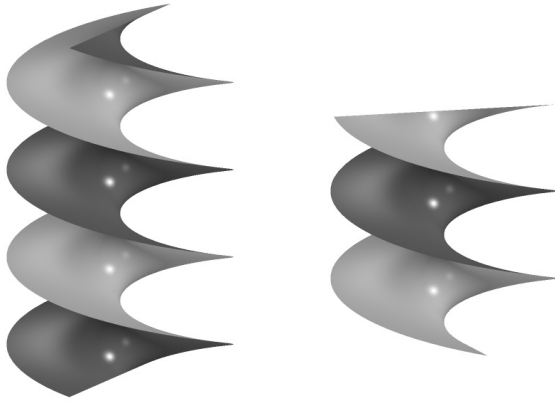


FIGURE 2. The Helicoid \mathcal{H} . On the right, the fundamental domain of \mathcal{H} modulo σ_k , for $k = 1.25$, is illustrated.

through $z \rightarrow e^{2i\theta} \bar{z}$), so its fixed-point set, which contains l , is a geodesic. Along l , $\frac{dz}{z}(\dot{l}) = 1/t$; hence $dh(\dot{l}) = i\lambda/t$ is imaginary, while $\frac{dg}{g}(\dot{l}) = k\frac{dz}{z}(\dot{l}) = k/t$ is real. From (2-1), we can conclude that the image of l lies in a horizontal plane, while from (2-7), it follows that the image of l is an asymptotic curve. Since it is a geodesic, it must be a horizontal straight line. Along $l(t)$, the metric (3-2) may be expressed as

$$ds = \frac{|\lambda|}{2}(t^{k-1} + t^{k+1})|dt,$$

from which it follows that the length of $l(t)$ diverges as $t \rightarrow \infty$ or $t \rightarrow 0$. Therefore, this is a complete metric on the punctured plane.

Remark 3.1. The form $dg/g = kdz/z$ is well-defined on $C - \{0\}$ and has simple poles at the end $E_0 := 0$ and $E_\infty := \infty$. Also, dh has simple poles at the ends. See (3-2) and Figure 3.

Inversion, $z \rightarrow \frac{1}{\bar{z}}$, is also an isometry of (3-2), so its fixed-point set, $|z| = 1$, maps into a geodesic. Parameterizing $|z| = 1$ by $\alpha(t) = e^{it}$, it is clear that $\frac{dz}{z}(\dot{\alpha}) = i$. Hence $dh(\dot{\alpha}) = -\lambda$ and $\frac{dg}{g}(\dot{\alpha}) = ki$. It follows from Equation (2-7) that the image of $|z| = 1$ is a straight

	E_0	E_∞
z	0	∞
g	0^k	∞^k
dh	∞	∞
$\frac{dg}{g}$	∞	∞

FIGURE 3. Divisors of the Weierstrass data for the Helicoid \mathcal{H} , modulo σ_k . The points E_0 and E_∞ correspond to the ends of the quotient surface.

line. Since $|z| = 1$ is orthogonal to a ray at every point, its image is orthogonal to a horizontal line at every point; it is a vertical line that we refer to as *the axis*.

For any angle θ , rotation by θ around 0, $z \rightarrow e^{i\theta}z$ is an isometry of (3-2). Hence, the angles that the horizontal lines on the surface make with the axis rotate at a constant speed. We are indeed looking at a helicoid. There is only one homotopy class on M' , whose representative we may take to be the unit circle, $|z| = 1$, on which dh has a nonzero real period of $-2\pi\lambda$. The one-form $dg/g = kdz/z$ satisfies $\int_{|z|=1} dg/g = 2\pi ik$. Therefore, the surface is invariant under a screw motion generated by a vertical translation by $-2\pi\lambda$ and a rotation about the axis by $2\pi ik$. We are free to scale the surface by varying the choice of the real number λ . To make the helicoid invariant under the screw motion σ_k defined in Section 1, we need to match the vertical translation, $-2\pi\lambda$, with the horizontal rotation $2\pi k$: We do this by choosing $\lambda = \pm k$ so that the vertical displacement,

$$\operatorname{Re} \int_{|z|=1} dh = -2\pi\lambda,$$

in one period is equal to $\pm 2\pi k$.

Remark 3.2. It is useful to note that we achieve the same choice of scaling, i.e., $\lambda = \pm k$, by requiring that the curvature of the helicoid be equal to -1 along the vertical axis. Indeed, from (2-6), when $|z| = 1$,

$$K = \frac{-16}{(|z|^k + |z|^{-k})^4} \frac{|kdz/z|^2}{|i\lambda dz/z|^2} = -\frac{k^2}{\lambda^2}.$$

In the next section, we will use this method of normalization.

4. WEIERSTRASS DATA FOR \mathcal{H}_k/σ_k

4.1 The Underlying Riemann Surface of \mathcal{H}_k/σ_k

Consider the torus represented by the equation,

$$w^2 = P(z) := z(z - e^{i\theta})(z - e^{-i\theta})(z - d), \quad (4-1)$$

where $0 < \theta < \pi$, and $d < 0$. The cross ratio of the roots of $P(z)$ is unitary. This property characterizes rhombic tori, the ones that are conformally equivalent to $\mathbf{C}/\{1, \tau\}$ with $|\tau| = 1$. The orientation-reversing involutions $(z, w) \rightarrow (\bar{z}, \bar{w})$ and $(z, w) \rightarrow (\bar{z}, -\bar{w})$ have the property that their fixed-point sets are closed curves that are the lifts of intervals on the extended real axis in the z -plane: the lift of $[d, 0]$ for $(z, w) \rightarrow (\bar{z}, -\bar{w})$; the lift of $[\infty, d] \cup [0, \infty]$ for $(z, w) \rightarrow (\bar{z}, \bar{w})$. These fixed-point sets

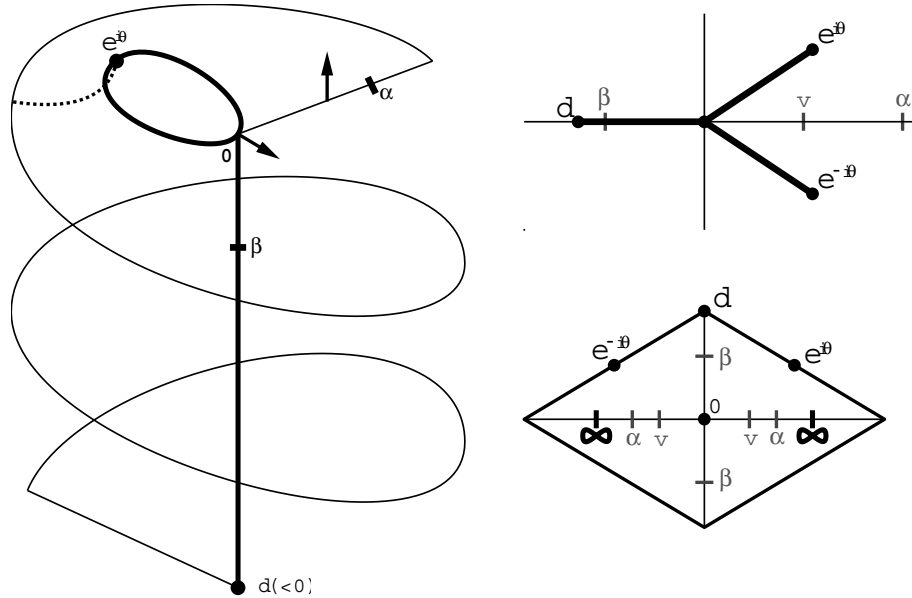


FIGURE 4. The geometric construction of the Weierstrass data for \mathcal{H}_k . Left: A sketch of a quarter of the desired surface \mathcal{H}_k . Top right: The z plane, over which Equation (4-1) defines a double covering branched at the points 0 , d and $e^{\pm i\theta}$. A lift of the upper halfplane corresponds to the quarter of the surface on the left. The segment $[0, d]$ corresponds to the vertical axis, the lift of the slit from 0 to $e^{i\theta}$ to the loop through corresponding points on in the sketch. Bottom right: The Riemann surface of (4-1) is a rhombic torus. Here that torus is illustrated as a planar domain. In all three diagrams, corresponding points are labelled by their z values in (4-1). The branch points of the covering (4-1) correspond to the fixed points of 180-degree rotation about the center of the rhombus on the lower right. These correspond in the sketch on the lefthand side to the fixed points of 180-degree rotation around the horizontal line through 0 and $e^{i\theta}$. The points on the right labelled v are positions of vertical points. The points labelled α and β correspond to the branch points. The relationship illustrated here of the branch points to the points corresponding to v and d is not forced on the computation. For $k = 1$, this is the correct relationship [Hoffman et al. 99]. Our computations indicate that these relations hold for $k > 1$, the regime of interest in this study. However, they do not hold for k near $1/2$.

can be considered to be the diagonals of a rhombus. (See Figure 4.) They cross at the points $(d, 0)$ and $(0, 0)$. The involutions above correspond to reflections across the diagonals. Without loss of generality, we will make the vertical diagonal correspond to the lift of $[d, 0]$.

We want to satisfy the conditions in (1-2), the characterization of \mathcal{H}_k . Condition (1-2(i)) requires the quotient of \mathcal{H}_k by σ_k to be a torus, and that torus will be the one described by (4-1). The vertical axis—required by condition (1-2 (iii))—will correspond to the vertical diagonal of the rhombus. The horizontal lines will correspond to the horizontal axis, which will be punctured twice at points corresponding to the ends of \mathcal{H}_k/σ_k . They will be placed symmetrically with respect to the center of the rhombus, a condition forced by the existence of a rotational symmetry around the vertical axis. This means that one of the horizontal lines crosses the axis at the point on \mathcal{H}_k/σ_k corresponding to the center, while the other horizontal line crosses at the point corresponding to the vertex of the rhombus. Weierstrass data that produces these geometric conditions must also satisfy (1-2(ii)). Namely,

the argument of the horizontal projection of the image of a closed curve around an end must increase by $2\pi k$.

4.2 Weierstrass Data in Terms of the Function z and w on the Torus

We develop candidate Weierstrass data in terms of the meromorphic functions z and w in (4-1). The function z on the torus is branched at the points $(0, 0)$, $(d, 0)$, $(e^{i\theta}, 0)$ and $(e^{-i\theta}, 0)$. (These points correspond to the center, the vertex, and the other two half-period points of the rhombus in Figure 4. They are in one setting the fixed points of the involution $(z, w) \rightarrow (z, -w)$, and in the other the fixed points of a 180-degree rotation about the center of the rhombus.) The one-form dz/w has no zeros or poles; it is equivalent, up to scaling, to the coordinate differential in the plane of the rhombus.

We will place the ends at the two points on the torus where $z = \infty$. Our construction of the torus $w^2 = P(z)$ in (4-1) with parameters d and $e^{i\theta}$ gives us a two-parameter family of tori, all rhombic. In fact, (d, θ) parameterizes the moduli space of symmetrically marked

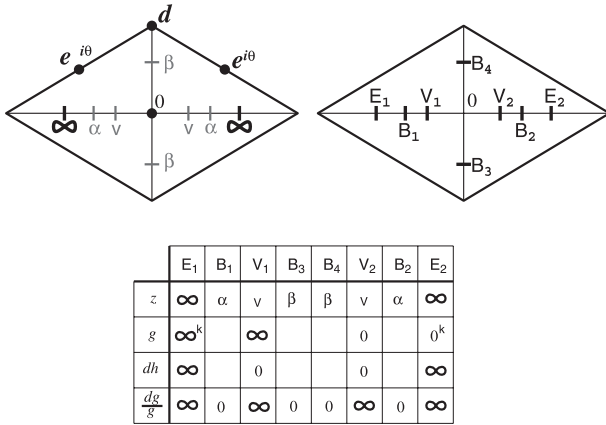


FIGURE 5. Tabulation of the Weierstrass data for \mathcal{H}_k .

rhombic tori. Our choice of representation, (4-1), also places the ends. (Each unmarked rhombus is represented by a one parameter family of pairs (d, θ) . It is straightforward to show that all rhombi with arbitrary placement of symmetric endpoints on the horizontal diagonal can be achieved by suitable choice of d and θ .) The pair of points on the horizontal diagonal where $z = \infty$ change with the choice of representation.

The function g on \mathcal{H}_k is the stereographic projection of the unit normal of \mathcal{H}_k . As observed before, unless k is an integer, g is not well-defined on \mathcal{H}_k modulo σ_k . However, dg/g does descend to the quotient. The Gauss map is vertical at the two ends, and—as on the helicoid— g has a simple zero at one end and a simple pole at the other. This forces dg/g to have a simple pole at the ends. (See Figure 3.) By Remark 2.1, dg/g will have additional poles at vertical points of g . But according to Remark 3.1 and Figure 3, if we want helicoidal ends, we must require dh to have a simple pole at the the ends. The zeros of dh correspond to vertical points, and since dh has no poles away from the ends and we are on a torus, this means there are precisely two vertical points on the surface. They can't be on the vertical axis (where the Gauss map is horizontal). By symmetry, there must be two simple vertical points that lie symmetrically on the horizontal diagonal. (If there is a vertical point off the diagonal, there would have to be at least four such points, an impossibility.) Again, since we are on a torus, dg/g must have four zeros corresponding to the branch points of g .

The helicoid has neither vertical points nor branch points, so we seek guidance for the placement of these points on \mathcal{H}_k from the singly periodic genus-one helicoid, \mathcal{H}_1 . This is natural enough, since we want the family \mathcal{H}_k

to include \mathcal{H}_1 when $k = 1$. We place two vertical points on the horizontal diagonal between the two ends, symmetrically placed on the segment that passes through the center. By the symmetry of rotation about the vertical diagonal, $g = 0$ at one vertical point and ∞ at the other. As on the singly periodic genus-one helicoid, the value of g coincides with the value of g at the end on the same side and the vertical point comes before any branch point as one travels from the center toward the end along the horizontal diagonal. This forces the existence of branch points between each vertical point and the end with the same value of g . We expect that (but do not require), as on \mathcal{H}_1 , the other two branch points will be symmetrically placed on the vertical axis.

The positioning of these points in the rhombus, and their correspondence with points on the surface (4-1) is given in Figure 4, and a tabulation of the divisor of dg/g based on the discussion in the previous paragraph is available in Figure 5. The lifts of the positive real axis form a curve on the surface through $(0, 0)$, which joins one end to the other. Therefore, the vertical points are placed at the two points on the surface where $z = v$ for some real $v > 0$. Similarly, the branch points on the horizontal line are located at the two points on the surface where $z = \alpha$, for α real. The two other branch points are located at the two points on the surface where $z = \beta < 0$, for β real. If $d < \beta < 0$, these points will be on the vertical axis; otherwise, they lie on a horizontal line.

Remark 4.1. In our calculation, we place the vertical points as described above and let that choice determine the location of the branch points. In fact, for $k \geq 1$, the branch points occur in the locations described above. However, for k near $1/2$, our computation indicates that the branch points leave the vertical axis and are located on the second horizontal line.

With this information, we are able to write dg/g :

$$\frac{dg}{g} = c \frac{(z - \alpha)(z - \beta)}{z - v} \frac{dz}{w} \tag{4-2}$$

Given a choice of α , β , and v , the value of c is determined by the requirement that g be well-defined in a neighborhood of a point where $z = v$, i.e., the residue of $\frac{dg}{g}$ is equal to $2\pi i$ at those points.

We will find it useful to express dg/g in a different form. Expanding $(z - \alpha)(z - \beta)$ in powers of $(z - v)$, we can write,

$$\frac{dg}{g} = (X + Y(z - v) + \frac{w(v)}{z - v}) \frac{dz}{w}, \tag{4-3}$$

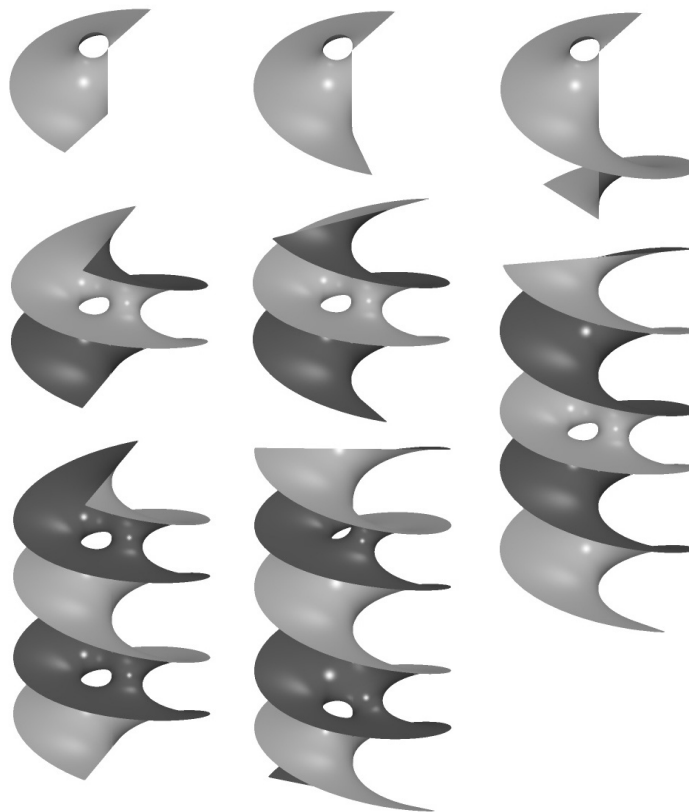


FIGURE 6. The surfaces \mathcal{H}_k . Left Column: The surface \mathcal{H}_1 ; on top, one quarter of the fundamental domain of \mathcal{H}_1 modulo σ_1 , corresponding to Figure 4, left; in the middle, one full fundamental domain containing four copies of the region above; on the bottom, two fundamental domains. Middle column: The surface \mathcal{H}_k for $k \sim 1.25$, with images that correspond to those in the first column. Right column: The surface \mathcal{H}_k for $k \sim 2.5$, with images corresponding to the top and middle images of the other two columns.

where X and Y are constants to be determined. The value $w(v)$ in the expression is again determined by the condition that g be well-defined in a neighborhood of a point where $z = v$, i.e., the residue of dg/g at $z = v$ equals 1. This form of dg/g will simplify the computation.

Remark 4.2. As for the helicoid in Section 3, the residue of dg/g determines the twist angle. From (4-3), the twist angle must be equal to $2\pi Y$.

The complex height differential dh must have a simple pole at the ends where $z = \infty$ and a simple zero at the vertical points where $z = v$,

$$dh = i\lambda(z - v)\frac{dz}{w}, \quad (4-4)$$

where λ is a nonzero real constant to be determined. We know that λ is real because dh must be imaginary along the positive real axis. (These points correspond to a horizontal line along which $x_3 = \operatorname{Re} \int dh$ is constant.)

Our desire to get a smooth deformation family of surfaces that behave like the helicoid leads us to our choice of the scaling factor λ . The vertical displacement of \mathcal{H}_k is given by the change in the x_3 coordinate at a cycle centered at an end, where $z = \infty$. From (4-4), it follows that the residue of dh at $z = \infty$ is equal to $-\lambda$. Hence, it is natural to choose $\lambda = \pm k$.

Remark 4.3. It is not possible to choose λ so that the curvature of \mathcal{H}_k is equal to -1 along the vertical axis. As noted in Remark 3.2, this scaling for the helicoid made it invariant under a screw motion.

However, we do not expect that the surfaces \mathcal{H}_k have constant curvature along the vertical axis; in fact, we expect *branch points* on this axis (where, by (2-6), $K = 0$). As a next-best choice, we could require $K = -1$ at the center point where $z = 0$.

Since the Gauss map is horizontal along the vertical axis, $|g(0)| = 1$. Using (2-6), we can compute K as we did in Remark 3.2:

$$K(0) = - \left| \frac{(X - Yv + \frac{w(v)}{-v}) \frac{dz}{w}}{-i\lambda v \frac{dz}{w}} \right|^2.$$

If $K(0) = -1$,

$$\lambda = |(X - vY - \frac{w(v)}{v})/v|.$$

This does not give $\lambda = k$, but it turns out to be relatively close. Because, as will be made clear in the next section, we solve for our surfaces as function of d and not of k , it is more practical to use this normalization for animations and images such as those in Figure 6.

4.3 Period Conditions

We can assume, without loss of generality, that the half-period points on the rhombus, which are fixed points of the normal involution corresponding to 180-degree rotation about its center, are mapped to points in R^3 at the same height as the image of the center point. Since the center point corresponding to the point where $z = 0$ and these fixed points correspond to the points where $z = \pm e^{i\theta}$, $Re \int_{\gamma} dh = 0$, where γ is the homological cycle lifted from the slit from 0 to $e^{i\theta}$. Using the expression for dh in (4-4), this condition determines the parameter v . Namely, $Re \int_{\gamma} dh = -\lambda Im \int_{\gamma} (z - v) \frac{dz}{w} = 0$, or

$$v = \frac{Im \int_{\gamma} \frac{z dz}{w}}{Im \int_{\gamma} \frac{dz}{w}}. \tag{4-5}$$

Since the image points of $z = e^{i\theta}$ and $z = 0$ are on the same x_3 level, we can calculate v via the integrals along the unit arc from $z = 0$ to $z = e^{i\theta}$. That is, v can be determined by the following condition:

$$Re \int_0^{\theta} \frac{(e^{i\phi} - v)d\phi}{\sqrt{\cos \phi - \cos \theta \sqrt{e^{i\phi} - d}}} = 0.$$

We may assume (after a rotation, if necessary) that $g(0) = 1$. For the Gauss map to be well-defined by (2-5), we require that

$$\int_{\gamma} \frac{dg}{g} = 2\pi i.$$

Using (4-3)(and simplifying using (4-5)), this condition produces a nondegenerate linear system that determines X and Y :

$$Im \int_{\gamma} \frac{dz}{w} X = - Im w(v) \int_{\gamma} \frac{dz}{(z - v)w} + 2\pi$$

$$Re \int_{\gamma} \frac{(z - v)dz}{w} Y + Re \int_{\gamma} \frac{dz}{w} X = - Re w(v) \int_{\gamma} \frac{dz}{(z - v)w}.$$

At this point, we are assured that the Gauss map is well-defined. We turn our attention to the remaining period problems for the Weierstrass integrals. Here the symmetry forced by the lines on the surface is of critical use. In (4-5), we have already killed the period for dh around the cycle corresponding to γ . We cannot and do not want to kill the period around the cycle corresponding to the vertical diagonal since this gives the translational part of the screw motion. So the vertical period problem (2-4) is solved. We now address the horizontal-period problem (2-3).

Our decision to rotate the surface so that $g(0) = 1$ forces the horizontal line through $X(0)$ to be mapped to a line parallel to the x_2 axis. This means that the x_1 -period in (2-3) is automatically solved. There is only one period left to be killed in (2-3), and that is the x_2 displacement along the cycle γ :

$$Im \int_{\gamma} (\frac{1}{g} + g) dh = 0. \tag{4-6}$$

If we choose d to be the free parameter in the representation of the torus in (4-1), the period condition (4-6) will determine the correct value of θ as a function of d . Therefore, we expect to have a one-parameter family of singly periodic minimal surfaces. The twist angle of the screw motion symmetry is determined by the residue of $\frac{dg}{g}$ at the end $z = \infty$, and we have noted in Remark 4.2 that its value is $2\pi Y = 2\pi Y(d)$.

5. NUMERICAL DATA AND FURTHER RESULTS

Numerical computation shows that for d ranging from -0.15 to large negative values, the value of θ decreases from ~ 2.29956 to ~ 1.25962 , and k grows without bound from an initial value close to $1/2$. (Recall that the twist angle equals $2\pi k$.)

In the cases of \mathcal{H}_1 and $\mathcal{H}e_1$, there are independent existence results ([Hoffman et al. 93, Hoffman et al. 99]) that also allow us to compute the rhombic invariants. The values we produce here are in accord with those independent computations.

When $d \sim 1.293$, the value of θ is approximately 1.48666 and we get $k = 1$. These are the parameters in (4-1) of the rhombus for \mathcal{H}_1 , the singly periodic genus-one helicoid of [Hoffman et al. 99]. In this case, the cross ratio of the roots of (4-1) is $e^{i\tau}$, with $\tau \sim 1.7205$. This, in turn, corresponds to a rhombus with a vertex angle of approximately 70.7083 degrees. As $d \rightarrow \infty$, the cross ratio of the roots of (4-1), using the limiting value

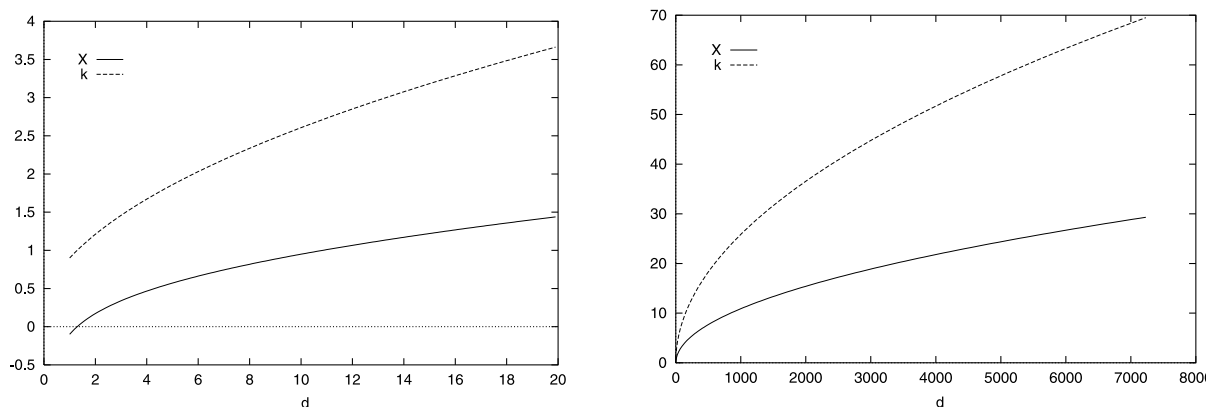


FIGURE 7. The twist angle k and the parameter X as functions of d . In these graphs the signs of d and k have been changed from negative to positive.

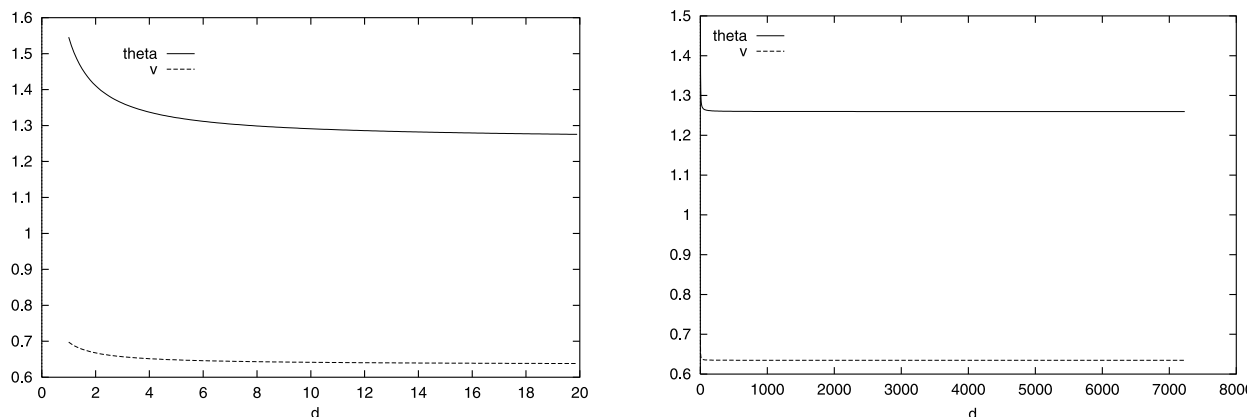


FIGURE 8. The conformal parameter θ and the parameter v that locates the vertical points. In these graphs, the sign of d has been changed from negative to positive. As d grows from 0.15 the value of θ decreases from 2.29956 to 1.25962, the latter value corresponding to the correct conformal parameter for $\mathcal{H}e_1$, the genus one helicoid of [Hoffman et al. 93]. It is evident from the graphs that the values of θ and v rapidly stabilize.

$\theta \sim 1.25962$, gives the appropriate value for the rhombic torus of $\mathcal{H}e_1$, the genus-one helicoid.

Images of three \mathcal{H}_k for three values of k are shown in Figure 6. Graphs of θ and v as functions of d are shown in Figure 7. Graphs of the twist angle k and the internal variable X are presented in Figure 8.

5.1 Computational Methods

It seems appropriate to say a few words about how these numerical values are computed. Reading Section 4 backwards, it is evident that for a fixed value of $d > 0$, a choice of θ determines w by (4-1), from which v is determined by the ratio in (4-5). Knowing v and w , we can compute the coefficients of the linear system for X and Y that precedes the displayed equation (4-6). Solving that system for X and Y , we can then use (4-3) to find g , and compute the integral in (4-6).

We want that integral to vanish, and we vary θ in order to achieve that numerically. The twist angle parameter k is determined, as explained in Remark 4.2, by the residue of dg/g at an end, which is simply Y . It is worth emphasizing that, while it is natural to think of the twist angle k as the natural parameter, our method required us to look at the conformal type of the underlying rhombus as the variable. From the forms of the integrals and equations we were solving, it was very reasonable to expect that the twist angle would be a continuous function of the conformal type.

The contour integrals were approximated by Gaussian quadrature, allowing us to avoid evaluation of the integrands at the endpoints of the paths, where they may be singular. As mentioned in the previous paragraph, we knew an accurate numerical value for θ when $d = d_1 \sim 1.293$, the value for the singly periodic genus-one heli-

coiled ($k = 1$). Varying d from this value, we used the previously computed value of θ as an initial approximation; the process converged rapidly for values of d greater than d_1 . However, for decreasing values, the process was less stable and reliable, as shown in Figure 7. It is worth noticing that we did not get much below d_1 . In fact, with more careful numerics, we could get fairly close to, but not below, a twist angle of $k = \frac{1}{2}$.

The images were made using MESH, a suite of programs written by James T. Hoffman (MSRI), which among other things provides automatic and tunable mesh generation for discretizing the surfaces under investigation. (See www.msri.org/publications/sgp/SGP/.)

5.2 The Limit as $k \rightarrow \frac{1}{2}$

A referee asked us to discuss the behavior of the family when the screw motion approaches the least possible value and wondered “Can the numerical approach give the answer?” The quoted question is one whose meaning is not as easy to grasp as it might seem at first glance. Depending on what is meant, the answer is either a muted “no” or a resounding “yes.”

At the time the computation was originally done, the authors clearly had in mind the idea that the family, if it existed, had as its limit as $k \rightarrow \infty$ a nonperiodic surface asymptotic to a helicoid and of genus one. That the computation gave screw-motion-invariant solutions for twist angles $2\pi k$, for values of k less than 1 was noted, as was the fact that the computation began to behave poorly as d approached values for which k was close to (but always greater than) $1/2$, and could not be pushed below $1/2$. For values of near $1/2$, the program MESH that does an automatic triangulation of the surface as it is being computed, slowed down significantly. We thought that it was likely that there was a numerical problem, that somewhere in the code we had implicitly assumed that $k \geq 1$ and that this contributed to the error. In retrospect, this was not very likely since—as explained above— k is an output of the computation. Still, some sort of poor parameterization could lead to errors like this, and we had seen behavior like this before. For example, at these extreme values, perhaps a branch point moved outside of a small circle used to compute a period. Also, the images of the surfaces for k near $1/2$ did not have any evident errors or telltale signs of impending degeneracy. The holes were not getting smaller, nor were they drifting away from the central axis. We were not prepared by any previous experience to take seriously the possibility that the family would stop at some surface that did

not appear to be degenerate. In fact, we hypothesized that it was possible for the twist angle to go to zero and imagined the holes getting smaller and smaller, closer together and clustering around the axis of the surface. The normalization of the surfaces in Remark 4.3 does not imply that the Gauss curvature is bounded as k goes to 0. The limit would have the handles lining up along the axis and shrinking down to zero to give, in the limit, the helicoid. This turned out not to be justified on the basis of what we saw and, from this point of view, the answer to the question, “Can the numerical approach give the answer?” is “No.”

It turns out that the numerics and the graphics were correct as far as they went, but this took additional development that was decidedly noncomputational in nature. Martin Traizet was a visitor to the GANG Laboratory in Amherst at the time we were doing these computations beginning in 1993. He was aware of the phenomena described in the previous paragraph. Some six years later, he developed a method of construction of minimal surfaces by a singular perturbation method, in which the Weierstrass representation and the implicit function theorem are used to solve the period problem. His first success in this area was to prove the existence of higher-genus Riemann examples, the originals of which had been computed by Wei [Traizet 02a]. He then extended this to construction of embedded minimal surfaces of finite total curvature. The idea was to consider the degenerate limit of known (computationally or theoretically) deformation families as an algebraic object that contained information about the position of degenerating catenoids in the family. He then showed that one could perturb slightly off the singular limit to produce Weierstrass representations, which—using an implicit-function theoretical argument—had all periods equal to zero ([Traizet 02b, Traizet 01]).

Traizet visited MSRI in the fall of 2000. Matthias Weber was at MSRI during that period and we discussed the possible limits of this family for small k . Weber noted that there were some reasons to expect that his alternate construction of the deformation family might fail at $k = 1/2$, and they discussed the possibility of extending Traizet’s ideas to this case. However, there were no degenerating catenoids in sight. Using Weber’s theta-function parametrization of these surfaces they were able to compute surfaces with a twist angle closer to π than we were. That made the difference. The images produced by MESH were quite revealing and unanticipated. With the aid of images like that of Figure 9, Traizet and Weber had the startling insight that this limit could be



FIGURE 9. Near the limit value $k = 1/2$. Screw-motion-invariant genus one helicoid with twist angle just slightly greater than π . The images here were produced with MESH using a representation of the surfaces under consideration that involves theta functions. This method was found by Weber [Weber 00] and implemented for use here by Traizet. Introduced for theoretical reasons, it also has computational advantages; it allows one to get much closer to $k = 1/2$. The surfaces shown here have $k = 0.501$.

considered to be degenerating into properly placed “half helicoids.”

This was, at first hard to credit but in fact, you can sort of “see” it in the pictures. Armed with this insight, they have been able to prove the existence near a singular limit (i.e., for k near $1/2$) of screw-motion-invariant helicoids of arbitrary genus [Traizet and Weber 02]. The images were crucial in obtaining this insight. In that sense, the answer to the question, “Can the numerical approach give the answer?” is certainly “Yes,” at least if one is in the right state of preparation to understand “the answer.” It took major theoretical advances of Traizet and Weber to get to that state (They were originally motivated by the numerical deformation experiments and then provided a better means of computing these surfaces very close to the critical twist angle of π .)

It is important to note, however, that Weber and Traizet do not show that there is degeneration as $k(d)$ approaches $1/2$. They show that there is a family with the same properties as the ones constructed here that does degenerate to a foliation by horizontal planes with three vertical lines of singularity. After rescaling, neighborhoods around these lines are close to helicoids. There is no uniqueness result: In particular, we do not know whether or not there is a family that extends past the value $d_{1/2}$ for which $k(d)$ approaches $1/2$. What happens, if anything, on the other side of $d_{1/2}$ is not known. The “numerical approach” used here is not going to tell us much about uniqueness.

In our opinion, the question, “Can the numerical approach give the answer?” is not well posed. The phrase “the numerical approach” is misleading. In this investigation a fair amount of theory is embedded in any compu-

tation. A picture of a computed minimal surface contains not only a visual means of understanding the computation, but also concealed theoretical information. It is not possible to understand what that picture means without a knowledge not only of how it was computed but why it was computed, and under what theoretical assumptions. The “experiment” described in this paper is neither numerical nor theoretical, but mathematical.

The authors are to be faulted for not publishing this paper earlier; for waiting until there existed a fuller theoretical justification for their investigations. They, too, did not see clearly enough through the misleading and limiting dichotomy of numerical vs. theoretical.

Acknowledgments

The visualization tools we used in this research were created by James T. Hoffman, who also produced the computer-generated images that illustrate this work. In the writing of this paper, we benefited from conversations with Matthias Weber and comments from Mike Wolf on an earlier version.

The authors wish to acknowledge the contribution of Hermann Karcher to the ideas and constructions in this paper. For years, as a collaborator, consultant and friend, we have benefited from his knowledge and his mathematical spirit.

Sections 5.1 and 5.2 were assessed in April 2002, in response to questions from the referees.

REFERENCES

- [Hoffman and Karcher 97] D. Hoffman and H. Karcher. “Complete embedded minimal surfaces of finite total curvature.” In *Encyclopedia of Mathematics*, pp. 5–93, R. Osserman, editor, Springer Verlag, Berlin-Heidelberg, 1997.

- [Hoffman et al. 93] D. Hoffman, H. Karcher, and F. Wei. “The genus one helicoid and the minimal surfaces that led to its discovery.” In *Global Analysis and Modern Mathematics*, pp. 119–170, edited by K. Uhlenbeck, Publish or Perish Press, Berkeley, CA, 1993.
- [Hoffman et al. 99] D. Hoffman, H. Karcher, and F. Wei. “The singly periodic genus-one helicoid.” *Commentarii Mathematici Helvetici* **74** (1999), 248–279.
- [Traizet 01] M. Traizet. “Construction of minimal surfaces by gluing weierstrass representations.” In *Proceedings of the Clay Mathematics Institute 2001 Summer School on the Global Theory of Minimal Surfaces*, D. Hoffman et al., editors, 2001.
- [Traizet 02a] M. Traizet. “Adding handles to the Riemann examples.” *Journal of the Inst. Math. Jussieu*, **1**:1 (2002), 145–174.
- [Traizet 02b] M. Traizet. “An embedded minimal surface with no symmetries.” Preprint, 2002.
- [Traizet and Weber 02] M. Traizet and M. Weber. In preparation, 2002.
- [Weber 00] W. Weber. *On the embeddedness of the genus one helicoid*. Habilitationsschrift, University of Bonn, 2000.
- [Weber 02] M. Weber. Period quotient maps of meromorphic 1-forms and minimal surfaces on tori. *J. Geom. Analysis* **12**:2, 2001.
- [Weber et al. 02] M. Weber, D. Hoffman, and M. Wolf. “An embedded genus-one helicoid constructed as the limit of periodic embedded minimal surfaces.” In preparation.

David Hoffman, MSRI, 1000 Centennial Drive, Berkeley, CA 94720 (david@msri.org)

Fusheng Wei, JMF Technologies, 5384 Harrow Lane, Fairfax, VA 22030 (fushengw@hotmail.com)

November 1, 2001; accepted March 27, 2002.